

Bubble Nucleation and Cooperativity in DNA Melting

S. Ares,^{1,2} N. K. Voulgarakis,³ K. Ø. Rasmussen,¹ and A. R. Bishop¹

¹Theoretical Division and Center for Nonlinear Studies, Los Alamos National Laboratory, Los Alamos, New Mexico 87545, USA

²Grupo Interdisciplinar de Sistemas Complejos (GISC) and Departamento de Matemáticas, Universidad Carlos III de Madrid, Avenida de la Universidad 30, 28911 Leganés, Madrid, Spain

³Department of Physics, University of Crete and Foundation for Research and Technology-Hellas (FORTH), P.O. Box 2208, 71003 Heraklion, Crete, Greece

(Received 5 October 2004; published 27 January 2005)

The onset of intermediate states (denaturation bubbles) and their role during the melting transition of DNA are studied using the Peyrard-Bishop-Dauxois model by Monte Carlo simulations with no adjustable parameters. Comparison is made with previously published experimental results finding excellent agreement. Melting curves, critical DNA segment length for stability of bubbles, and the possibility of a two-state transition are studied.

DOI: 10.1103/PhysRevLett.94.035504

PACS numbers: 63.20.Pw, 87.15.He

Accessing the genetic code stored in DNA is central to fundamental biological processes such as replication and transcription, and this requires that the extraordinary stable double helical structure of the molecule must locally open to physically expose the bases. Although, in the cell, proteins may actively help separating the strands of double-stranded DNA, recent evidence [1,2] corroborates that sequence-specific propensity to form strand separations (bubbles) at transcription initiation sites exists and promotes thermal bubble formation. Important thermal effects such as stability of different DNA sequences, and the properties of denaturation bubbles, can be studied *in vitro* and provide important insight into the biological processes. Recent experimental studies [3–5] have attempted to interrogate the nature and statistical significance of such bubble states. Intriguingly, these experiments combine traditional UV absorption experiments with a novel bubble quenching technique that traps ensembles of bubbles to capture statistical properties of the bubbles.

The actual melting of double-stranded DNA occurs through an entropy-driven phase transition. The entropy gained in transitioning from the very rigid double-stranded DNA to the much more flexible single-stranded DNA can, already at moderate temperatures, balance the energy cost of breaking a base pair. Since the double-stranded helix is held together by hydrogen bonds between complementary base pairs—two bonds for the adenine-thymine (AT) pair and three bonds for the stronger guanine-cytosine (GC) pair—the sequence heterogeneity interplays with the entropy effects to create an extended premelting temperature window (including the biologically relevant regime), where large thermal bubbles are readily formed. Theoretical studies of the melting transition have included ones based on Ising-type models [6] describing paired and unpaired bases, thermodynamic models like nearest-neighbor models [7], Poland-Scheraga models [8], simple zipper models [9,10], or models that introduce a phenome-

logical pairing potential between the bases [11–13]. In particular the Peyrard-Bishop-Dauxois model [12,13] is emerging as a model that is able to appropriately describe the melting transition but also the sequence dependence of the bubble nucleation *dynamics* in the premelting regime.

Here, we compare the powerful recent experimental results in Refs. [4,5] with Monte Carlo simulations of the

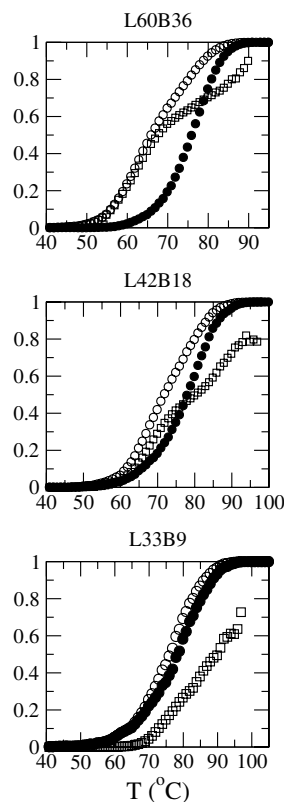


FIG. 1. Melting profiles for the *bubble-in-the-middle* sequences [3–5]. Filled circles are p , open circles are f , and squares are l .

model proposed by Peyrard, Bishop, and Dauxois [11–13]. This model has already been successfully compared with denaturation experiments on short homogeneous sequences [14]. The recent demonstration [1] of the model's ability to accurately predict the locations at which large bubbles form in several viral sequences is even more exceptional. The difference between our comparison and previous ones is that we use the same (deceptively) simple model, with no further refinements that introduce new parameters that need to be fitted. Indeed parameters of the model are not changed to fit the experiments: we use the *same* values for those parameters that were fixed in Ref. [14] for quite different DNA sequences.

The potential energy of the model reads

$$V = \sum_n \left[D_n (e^{-a_n y_n} - 1)^2 + \frac{k}{2} (1 + \rho e^{-\beta(y_n + y_{n-1})}) (y_n - y_{n-1})^2 \right]. \quad (1)$$

The sum is over all the base pairs of the molecule and y_n denotes the relative displacement from equilibrium at the n th base pair. The first term of the potential energy is a Morse potential that represents the hydrogen bonds between the bases. The second term is a next-neighbor coupling that represents the stacking interaction between adjacent base pairs: it comprises a harmonic coupling multiplied by a term that strengthens the coupling when the molecule is closed and makes it weaker when it is melted, in this way taking into account the different stiffness (i.e., entropy effects) of DNA double strands and single strands (this effect can be directly observed, in model calculations, in terms of a softening of the characteristic frequencies of the system with rising temperature [15]). This nonlinear coupling results in long-range cooperative effects in the denaturation, leading to an abrupt entropy-driven transition [12,13]. A crucial point for obtaining correct results is the accurate description of the heterogeneity of the sequence [16]. In this model it is incorporated by giving different values to the parameters

of the Morse potential, depending on the base-pair type of the site considered: AT or GC. The parameter values we have used are those used in Ref. [14]: $k = 0.025 \text{ eV}/\text{Å}^2$, $\rho = 2$, and $\beta = 0.35 \text{ Å}^{-1}$ for the intersite coupling, while for the Morse potential $D_{\text{GC}} = 0.075 \text{ eV}$ and $a_{\text{GC}} = 6.9 \text{ Å}^{-1}$ for a GC base pair, and $D_{\text{AT}} = 0.05 \text{ eV}$ and $a_{\text{AT}} = 4.2 \text{ Å}^{-1}$ for an AT pair. These parameters were chosen to fit thermodynamic properties of DNA [14]. One should be cautious in relating these parameters directly to microscopic properties, and recall that they arise as a result of several physical phenomena at the microscopic level.

Using the standard Metropolis algorithm [17,18], we have performed Monte Carlo simulations on this model [19]. For each temperature, we performed a number of simulations. In each of these simulations, we compute the mean profile $\langle y_n \rangle$, from which we obtain the fraction of open base pairs. We consider the n th base pair to be open if $\langle y_n \rangle$ exceeds a certain threshold. Applying the same threshold, we record at the end of each simulation whether the entire molecule was open (denaturated). Performing a large number of such simulations starting from different initial conditions we obtain the averaged fraction f of open base pairs and the averaged fraction of denaturated molecules p at a given temperature. In this way, we “simulate” the experiments, where the measures are made over a large ensemble of molecules. The threshold we have used is 0.5 Å, but we have used other values and observed that the fraction p of denaturated molecules depends only very slightly on the threshold value. The fraction of open base pairs, f , displays a somewhat stronger dependence on the threshold value. In the same manner as Ref. [4] we obtain the averaged fractional length of the bubbles as $l = (f - p)/(1 - p)$. The experimental work [4,5] concentrated on two sets of sequences: one set (*bubble-in-the-middle* sequences) designed to form bubbles in the middle of the short sequence, and another set (*bubble-at-the-end* sequences) designed to form bubbles (openings) at one end of the sequences. Specifically, these sequences are:

(a) *Bubble-in-the-middle sequences.*

L60B36: CCGCCAGCGGCGTTATTACATTTAATTCTTAAGTATTATAAGTAATATGGCCGCTGCGCC

L42B18: CCGCCAGCGGCGTTAATACTTAAGTATTATGGCCGCTGCGCC

L33B9: CCGCCAGCGGCCTTTACTAAAGGCCGCT GCGCC

(b) *Bubble-at-the-end sequences.*

L48AS: CATAACTTTTATATTTAATTGGCGGCGCACGGGACCCGTGCGCCGCC

L36AS: CATAACTTTTATATTGCCGCGCACGCGT GCGCGGC

L30AS: ATAAAATACTTATTGCCGCGCACGCGT GCGGC

L24AS: ATAATAAAATTGCCCGGTCCGGGC

L19AS2: ATAATAAAGGCCGTCCGCC.

The bubble-in-the-middle sequences are rich in AT base pairs in the middle, while the bubble-at-the-end sequences are rich in AT base pairs at one end of the molecule. The AT base pairs are bonded by two hydrogen bonds, as opposed to the

stronger triple hydrogen bonding of the GC base pairs. This fact is obviously reflected in the model parameters ($D_{AT} = 0.05$ while $D_{GC} = 0.075$) and it also indicates that AT-rich regions denature at lower temperatures than GC rich regions.

In Fig. 1 we present our results for the bubble-in-the-middle sequences and we see a very good agreement with the experimental results given in Refs. [4,5]. As in the experimental results, we find for the L60B36 sequence that $f \approx l$ for $l < 0.6$. After this point, l displays a plateau, resulting from the occurrence of completely denaturated molecules at $T \approx 65^\circ\text{C}$. As noted in the experimental work, the plateau occurs at $l \sim 0.6$ because this is the ratio between the AT-rich central region, of 36 base pairs, and the molecule's total of 60 base pairs. The fact that $f \approx l$ before the plateau indicates that the bubble opens continuously as a function of temperature until it reaches its full size, while there are very few completely melted molecules at these temperatures. For the L42B18 sequence we again find a plateau in l at the value $42/18 \approx 0.43$, but here $f \neq l$ even at the lower temperatures (this is even more pronounced for L33B9). This shows that bubble generation and complete denaturation are both possible at lower temperatures. Since the three sequences are similar in structure and merely differ in the length of AT-rich region, this demonstrates that for these structures bubbles are only sustainable if the soft region is of size 20 base pairs or

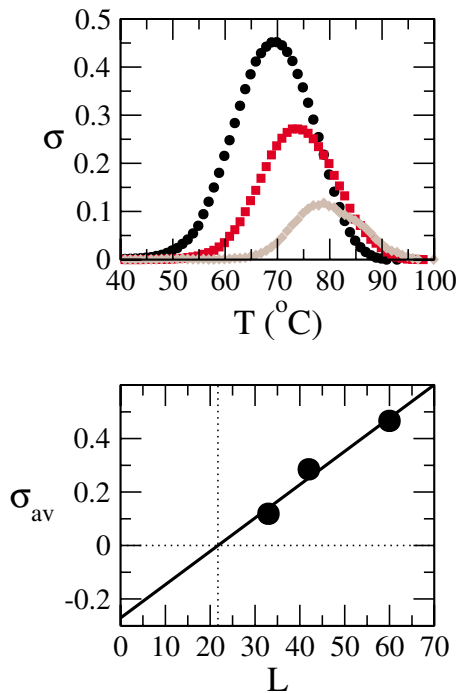


FIG. 2 (color online). Upper figure: $\sigma = f - p$ vs T for L60B36 (circles, upper curve), L42B18 (squares, middle curve), and L33B9 (diamonds, lower curve) [3–5]. Lower figure: σ_{av} vs the length, L , of the molecule.

more. To further illustrate this point we show in Fig. 2 $\sigma = f - p$, which represents the fraction of bases participating in a bubble state at a given temperature. The upper figure of Fig. 2 shows, as discussed, that as the soft bubble region becomes shorter, bubble states become less important, as also seen in Ref. [4]. In the lower figure, we summarize the length dependence of the incidence of bubble states. We plot σ_{av} , the area under the curves in the upper figure divided by their width, versus the molecule length, L . The line is a linear fit showing that these intermediate states disappear ($\sigma_{av} = 0$) for $L \approx 22$, in excellent agreement with the experimental conclusion in Refs. [4,5].

In Fig. 3 we show the melting curves for two of the bubble-in-the-end molecules. Comparison with experimental results in Ref. [5] is again good although not as good as in the bubble-in-the-middle cases. This is due to the limitations of our model at the ends of the DNA molecule. Most experimental features are, however, still reproduced. For instance, in the L48AS sequence we find the same plateau on l at $L \approx 0.8$ that is seen in the experiments. To overcome the problem caused by the boundaries, in Fig. 4 we consider how σ and σ_{av} change with the system size, as the deformation imposed by the excessive end opening will appear in all the molecules and in that way will not contaminate the global picture. In the upper figure we plot σ vs $T - T_m$ (T_m is the melting temperature), finding that the bubble states are smaller for the shorter sequences, as in Ref. [5]. In the lower figure we plot σ_{av} vs L . The extrapolation to $\sigma_{av} = 0$ occurs at a

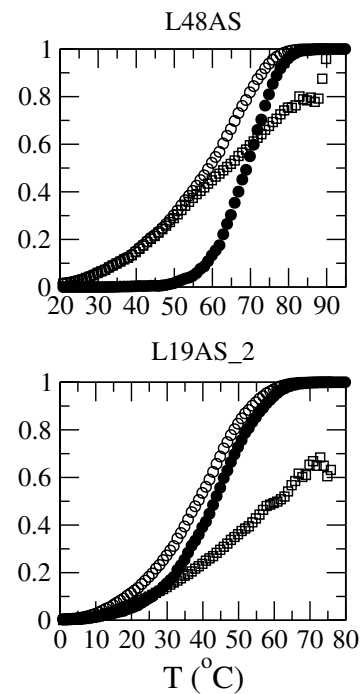


FIG. 3. Melting profile for the L48AS and L19AS_2 sequences. Symbols are as in Fig. 1.

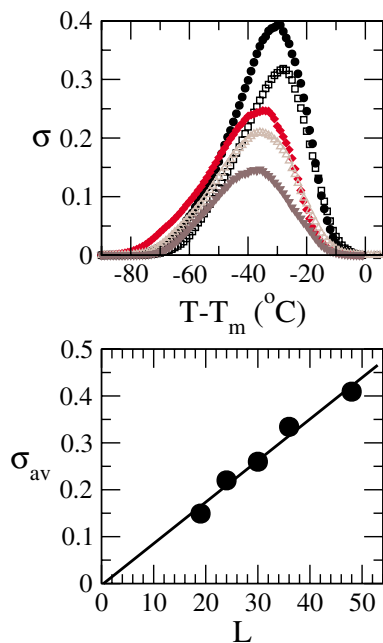


FIG. 4 (color online). Upper figure: $\sigma = f - p$ vs $T - T_m$ (T_m is the melting temperature) for L48AS (circles, top curve), L36AS (squares, second curve from top), L30AS (diamonds, third curve from top), L24AS (up triangles, second curve from bottom), and L19AS_2 (down triangles, bottom curve) [3–5]. Lower figure: σ_{av} vs L , the molecule's length.

value compatible with $L \approx 1$, as in Ref. [5], and shows that in our model a two-state transition for this kind of sequence would only be possible in the limit $L \approx 1$, just as in the experiments.

We have shown that the theoretical model proposed by Peyrard, Bishop, and Dauxois, with no further parameters or fitting, accurately reproduces experiments on DNA denaturation, not only for the melting curve, but also for the formation and role of bubble states in the premelting regime. Experimental observations regarding nucleation size of the bubbles in the middle of a molecule and the possibility of a two-state transition are exactly recovered by the model. This demonstrates that this model not only works for very large DNA strands [1], but also for short strands such as the ones studied here. Remarkably, these include both natural and synthetic structures.

We are grateful to Professor G. Zocchi for insightful discussions of the data in Refs. [3–5]. This work has been supported in part by the Ministerio de Ciencia y Tecnología of Spain through Grant No. BFM2003-07749-C05-01 (S.A.). S.A. acknowledges financial support from the Center for Nonlinear Studies, where this work was per-

formed. Work at Los Alamos is performed under the auspices of the U.S. Department of Energy.

-
- [1] C. H. Choi *et al.*, *Nucleic Acids Res.* **32**, 1584 (2004).
 - [2] G. Kalosakas, K. Ø. Rasmussen, A. R. Bishop, C. H. Choi, and A. Usheva, *Europhys. Lett.* **68**, 127 (2004).
 - [3] A. Montrichok, G. Gruner, and G. Zocchi, *Europhys. Lett.* **62**, 452 (2003).
 - [4] Y. Zeng, A. Montrichok, and G. Zocchi, *Phys. Rev. Lett.* **91**, 148101 (2003).
 - [5] Y. Zeng, A. Montrichok, and G. Zocchi, *J. Mol. Biol.* **339**, 67 (2004).
 - [6] M. Ya. Azbel, *Phys. Rev. A* **20**, 1671 (1979), and references therein.
 - [7] J. Santa Lucia, Jr., *Proc. Natl. Acad. Sci. U.S.A.* **95**, 1460 (1998).
 - [8] D. Poland and H. A. Scheraga, *J. Chem. Phys.* **45**, 1456 (1966); **45**, 1464 (1966); D. Poland, *Biopolymers* **73**, 216 (2004); C. Richard and A. J. Guttmann, *J. Stat. Phys.* **115**, 925 (2004).
 - [9] C. Kittel, *Am. J. Phys.* **37**, 917 (1969).
 - [10] V. Ivanov, Y. Zeng, and G. Zocchi, *Phys. Rev. E* **70**, 051907 (2004).
 - [11] M. Peyrard and A. R. Bishop, *Phys. Rev. Lett.* **62**, 2755 (1989).
 - [12] T. Dauxois, M. Peyrard, and A. R. Bishop, *Phys. Rev. E* **47**, R44 (1993).
 - [13] T. Dauxois and M. Peyrard, *Phys. Rev. E* **51**, 4027 (1995).
 - [14] A. Campa and A. Giansanti, *Phys. Rev. E* **58**, 3585 (1998).
 - [15] N. K. Voulgarakis, G. Kalosakas, K. Ø. Rasmussen, and A. R. Bishop, *Nano Lett.* **4**, 629, (2004).
 - [16] S. Ares and A. Sánchez (to be published).
 - [17] N. Metropolis *et al.*, *J. Chem. Phys.* **21**, 1087 (1953).
 - [18] We use the standard Metropolis algorithm to produce an equilibrium state of the system: A single base pair, n_0 , is picked at random and a new value of the variable y_{n_0} is proposed according to a thermal (at the appropriate temperature) Gaussian distribution at this base pair. The proposed value is accepted according to the Metropolis probability: 1 if the energy E_{new} of the new configuration is lower than the energy E_{old} of the old configuration, and $\exp(-[E_{new} - E_{old}]/kT)$ if $E_{new} > E_{old}$. The process is continued after thermal equilibrium is reached in the measurement phase.
 - [19] We have used periodic boundary conditions for the bubble-in-the-middle sequences and open boundary conditions for the bubble-at-the-end sequences. While it may appear most reasonable to apply open boundary conditions, in both cases, we consistently find that such boundary conditions lead to a much too large propensity for openings at the ends of the DNA molecule. This represents a clear problem of the model that we are working towards improving.